# SUPPLEMENTAL INFORMATION

## Supplemental Figure 1

**A** >DOT1L; human; range -1000bp to 100bp.

TACCTCAGCCCCCGCAGTAGCTGGGATTACAGGCGCCCGCCACCGCGCCCAGCTAATTTTTGTATTTTTA
ATAGAGACAGGGTTTCACCATGTTGGCCAGGCTGATCTCGAACTCCTGACCTCAGGTGATCTTCCCGCCT
CGGCCTCACAAAGTGCTGGGATTACAGGCATGAGCCAGGGCTCCTGGCCGTGAGAGGGGGTTTCTCCATG
TTGGTCAGGCTGGTCTCGAACTCCTGACCTCAGGTGATCTGCCCGCCTTGGCCTCCCAAAGTGCTGGGAT
TACAGGGGTGAATCACCGCGCCTGGCCTTTTTTTTTTTTTTTGTACCCAATAAACAGCATTGTTGTCGAA
TGAATACTGGACTTGGAGCTACAGCAAGTCCTGGACCGTGACTCTTATGGGGGGAAATTCGGATTTTTGG
TTTTACTAAGCCGTGTGTGGGGAGGTGTCCGGCGTCCTCCTCCTGGGACGGGATTCGAACCCGCTATCCG
ACGGGCCCGCCCACAGGGTCTCCCCGGGTCCCCGCTTCGGGCCGGCGAGTGGGGGAAGGGGTCGGCCGAG
GGCAACCGAGGACGTGCGTGCGTACGTTCGTGCGTGCGTGGATTCGGGCGGGCGGGCGAGTCCACGGGGC
GGGGCGCCGAGGGGGTGGCGCGCGCGGGTCGGCCCGCTGGGCGGCGGGCACGCGCCGGCGTCTTCGCTCC
GGGCTCCCCTAGCGCGCGGGGCGAGTGGTTCCGCCCGGCCCCCGGCTCATTGTGCTCGCTTCACGCCGGC
CCAAGATGGCGGAGGCGCTGGAGGCCCCGGGCCTGTGACTACAAAGAGGGAGTCGGGGGCCGGGCCGGAC
CGGAGCGCGGCGGCGGCGGCGGCGGCCGAGGCCGAGGCCAGGCCCCCTCCCCTCAGCCTCCCGCCCC
TCCCTCCCGCCCGCCCTCCTCCGCCCACCGGCGGCCCCGCCCCTCCCCCAACCGCCCGCCTAGCATGGTG
CGGCGGCCGCGCGCGCGGACATGGGGGAGAAGCTGGAGCTGAGACTGAAGTCGCCCGTGGGGGCTGAGCC
CGCCGTCTACCCGTGGCCGCTGCCGGTCTACGTGAGTGCCGCCCTCCACCG

**B** >DOT1L; mouse; range -1000bp to 100bp.

TTCTAGCTCCGGATCCTTCTTTTGGGGGCTGGCAAGCGCTAGGATGAGGGGTGGGAGCCATCTCCCCTAG
ATTACATTCACTCCCATGTAGTCAGGAAGAAGAAGCAGCTATCCAGAAGCGGCTGGTGAGCTGGTGACAG
CTCACCTCAAGGTAACTTATTCTCAGAAGGTTTTGGGGGGAGGGAACTTAAGTATTAGAAGGATTGGAAT
GGCCTAAGAAGGAAATAAGTTTGGCTCCTGACTCTGTAAAGTTCTGGGCAGGTCAGAGAATAACATTGCT
TTGAACTCTTAATTGAGAGCCTCCGACCTATAGGGTCCAATTTGACTGATGATTTATTAATTAACTTATT
GCTCACATCTTTAATCCCAGCTCTCAGGAGGCAGAGGCAGGTGGATTTTGGTAAATTCGAGGTCAGACTG
GTCAACAGAATGAGTTCCTGGACAGCCAGGGACACCCTGTCTCAAAAAAAAAAAAAAAAAAAAAGCATG
TAAATAAACAATAAGCAGATAGGCTAGAAAAGTGAAAAAATAGAAAAGCTAAAGAAGGGGAAAAATTGAA
AAATGAAAAAAAAAAGAAAGAAAGAAAAAGCCAGAAAAACAGAAAAAGAAAATTGACGGGAAGGGAAGAG
AAAGAAAAAGAACAGGAAATGGAAAGAAAAGAAAAAAGCAAAGCAAAGCGAAGGGACGCGAAGCAAGCCT
GTGCAACTGGGATTTGAACTTGACCCCGCCTGGTCTCTCTCGCTTTCCTCCGCAGGGTTTCCCCGGGTCC
CCGCTTCCGGCTGGCGGCGACGTCGGAGGGCAACCGAGGACGTGCGTGCGCCGCTGCGTGCGTAAGTGCG
TGCGTCGGTCGGAGGAGGGCGAGTCCAAGGGGGCGTGGCGTGCGAGGGGTGGCGCGCGCGGCGCGGCGGG
CGGAGGCTCTGGGCGCGCACCGCCTCTTGGCTCCCGGCCTCCCCCGCGCGCGCTCGCCGAGTGGTTCCGC
CCGACCCCCCGGCTCATTGTGCCTTCTCCTCACGCCGGCCCAAGATGGCGGCGGCTCTAGACGCCCCGGC
TCTGTGACTCCTACAAAGAGGGGAGCTGGGGCCACACGGGAGCGGCGGCCG

**C** >DOT1L; rat; range -1000bp to 100bp.

ATGTATGTTTATGCACCACGATTGCCTGGTGCATGGAGAGGCCAGAAGAGGGCGTTGGAACCCTGGGAAT
TCAGTCAGAGATGGTTGTGAGCCCGAGGGAGGGCTGGGAATGGAATCTAAGGTTCTCTAAAAGAGCAGCC
TGTAGTCTTAGCTACTGAACCATCTCTCTAACCCATTTGATGATTTTGTTTTTCAGTTTTGTTCTTGCTG
TTAGGAATGGTTTCACTCTGTAGCTCAAGTGGGCTTTGAGTCGTGATCCCTTGCCTCAGCTTCCCAAGAC
CTTGGATTATGGGTCATAGATTCACGGTTTTGTTAGTGTGAAACTGCATAGAAAGTCGGAAAATATCTTC
AAAAAGAATGAAAAGAAGCTAGGCGTGGGTGGTGCACACCTTTAATCCCAGCACTAGGGAGGGAGGCAGAG
GCGGGGAATCTTGGTGAATTTGAGGTAAGACTGGTCAACAGAGTAGACGGAGTTCCAGGACAGCCAGGGC
TACCGTGTCTCAAAAAAAAAAAAAAAACCAAATAAGTAAATAAACAATAAATAAGTGGATAAGATAAAAA
AAAGTGAAAAGAGAAACAGAAAAAGGAAAAAAGCCGGAAAAACAGAAAAAGAATAGGGACGAGAAGAGAA
AGAAAAGGAAAAGGAAAGGAAAGAAAAGAAAAAGAAAAGAAAAGAAAAAAAAGCAAAGCAAAGCGAGCCT
GCGCAACTGGGACTTGAACTTGTCCCCACCTGGTCTCTCTCGCTTGCCTCAGCAGGGTTTCCCCGGGTCC
CCGCTTCCGGCTGGCGGTGGCGTCGGAGGGCAACCGAGGACGTGCGTGCGACCCTGCGTGCGACGTGCG
TGCGTCGGCGGGAGGTGGGCGAGTCCAAGGGGGCGTGGCGTACGAGGGGTGGTGCGCGCGGCGCGGCGGG
CGGAGGCTTTGGGCGCGCACCGCCTCTTGGCTCCCGGCCTCCCCCGCGCGCGCGCGCCCAGTGGTTCAGC
CCGACCCCCCGGCTCATTGTGCCTTCTCCTCACGCCGGCCCAAGATGGCGGCGGCGCTAGACGCCCCGGC
TCTGTGACTCCTACAAAGAGGGGAGCTGGGGCCACACGGGAGCGGTGGCCG

**Supplemental Figure 1** Predicted hypoxia response elements (HREs) in human, mouse and rat *DOT1L* gene promoters. (A-B-C) Sequences of the human (A), mouse (B) and rat (C) *DOT1L* gene promoters from 1000 base pairs (bp) upstream of the transcription start site (TSS) to 100 bp downstream of the TSS as determined by the Eukaryotic Promoter Database. HREs with core consensus sequence 5'-(A/G)CGTG-3', potential binding sites for HIF heterodimers, are marked with a yellow box. The bp downstream of the TSS are highlighted in grey.

# Supplemental Figure 2

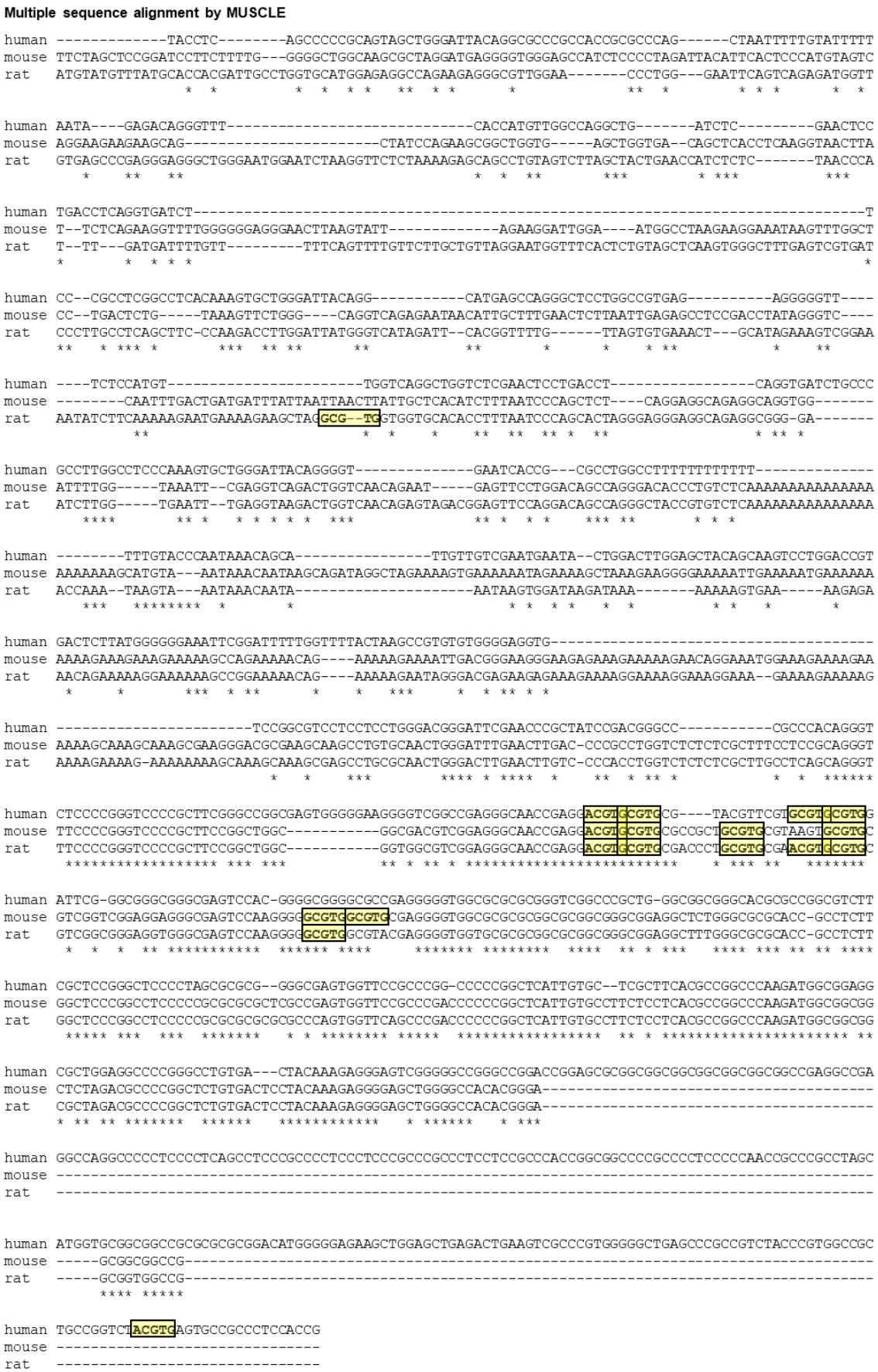

**Supplemental Figure 2** Alignment of the human, mouse and rat *DOT1L* gene promoters. Alignment of the human, mouse and rat sequences of the *DOT1L* gene promoters from 1000 base pairs (bp) upstream of the transcription start site (TSS) to 100 bp downstream of the TSS as determined by the Eukaryotic Promoter Database. This alignment was performed using MUSCLE. Hypoxia response elements (HREs) are marked with a yellow box.

**Supplemental Figure 3**

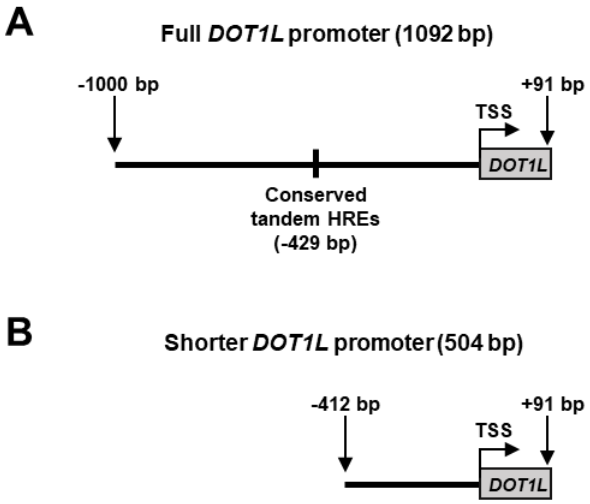


**Supplemental Figure 3** Promoter constructs for the luciferase reporter assay. (A) The full human *DOT1L* promoter from 1000 base pairs (bp) upstream to 91 bp downstream relative to the transcription start site (TSS) as defined by the Eukaryotic Promoter Database was cloned into the pGL3 basic luciferase reporter vector. This 1092 bp fragment contains the conserved overlapping tandem Hypoxia response elements (HREs) located at -429 bp relative to the TSS. (B) The shorter *DOT1L* promoter from 412 bp upstream to 91 bp downstream relative to the TSS was cloned into the pGL3 basic luciferase reporter vector. This 504 bp fragment does not contain the conserved overlapping tandem HREs.

**Supplemental Figure 4**

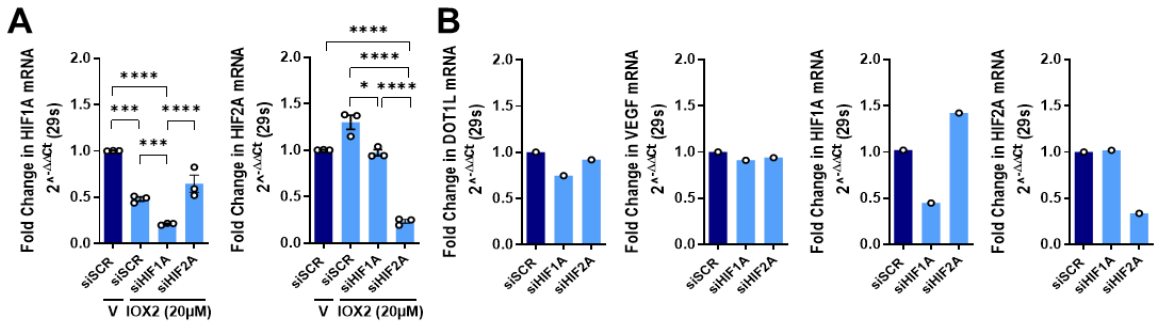


**Supplemental Figure 4** Efficiency of siRNA-mediated gene silencing in C28/I2 cells. (A) Real-time PCR analysis of *HIF1A* and *HIF2A* in human articular chondrocyte C28/I2 cells after treatment with hypoxia mimetic IOX2 (20 µM) and siRNA-mediated silencing of *HIF1A* (siHIF1A), *HIF2A* (siHIF2A) or scrambled control (siSCR) (n=3, **p*<0.05, ****p* <0.001, *****p*<0.0001 Sidak-corrected for 6 tests in one-way ANOVA). (B) Real-time PCR analysis of *DOT1L*, *VEGF*, *HIF1A* and *HIF2A* in C28/I2 cells after siRNA-mediated silencing of *HIF1A*, *HIF2A* or scrambled control (siSCR) (n=1). Bar graphs are mean±sem.

**Supplemental Figure 5**

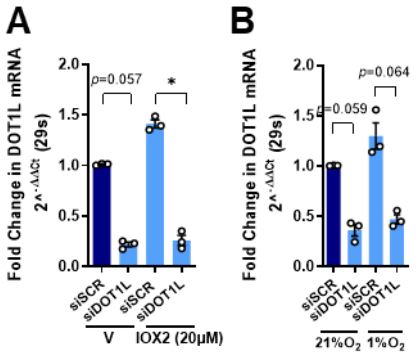


**Supplemental Figure 5** Efficiency of siRNA-mediated gene silencing in hACs. (A-B) Real-time PCR analysis of *DOT1L* in primary human articular chondrocytes (hACs) after treatment with hypoxia mimetic IOX2 (20 μM) or vehicle (V) (A) (n=3, **p*<0.05, Sidak-corrected for 6 tests in two-way ANOVA) or culturing in hypoxic conditions (1% $O_2$) (B) and siRNA-mediated silencing of *DOT1L* or scrambled control (siSCR) (n=3, Sidak-corrected for 6 tests in two-way ANOVA). Bar graphs are mean±sem.

**Supplemental Figure 6**

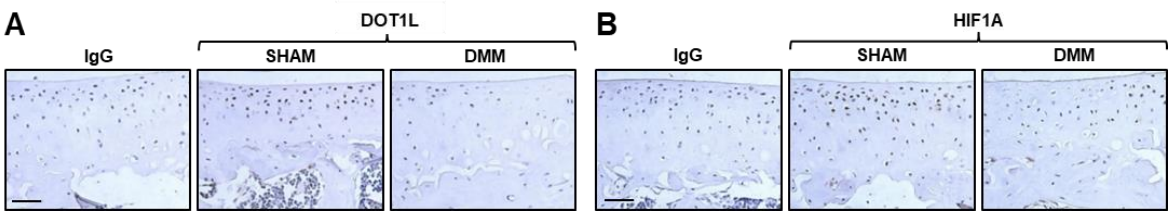


**Supplemental Figure 6** DOT1L and HIF-1A protein levels in osteoarthritis murine articular cartilage. (A-B) Immunohistochemical detection of DOT1L (A) and HIF1A (B) in the articular cartilage of wild-type mice with OA triggered by destabilisation of the medial meniscus (DMM) surgery compared to sham operated mice. The images are representative of three different animals. Scale bar, 50 µm.

**Supplemental Table 1**

**Human primers used for qPCR**

| Primer name | Sequence |
|---|---|
| **hACAN_fw** | ATCCGAGACACCAACGAGAC |
| **hACAN_rv** | CACTCATTGGCTGCTTCCTG |
| **hCOL2A1_fw** | TGGCAGAGATGGAGAACCTG |
| **hCOL2A1_rv** | CATCAAATCCTCCAGCCATC |
| **hDOT1L_fw** | GGATCTCAAGCTCGCTATGG |
| **hDOT1L_rv** | GTCGATGGCACGGTTGTACT |
| **hHIF1A_fw** | TCATCCATGTGACCATGAGG |
| **hHIF1A_rv** | TTCCTCGGCTAGTTAGGGTACA |
| **hHIF2A_fw** | CTGCGACCATGAGGAGATTC |
| **hHIF2A_rv** | GTACGGCCTCTGTTGGTGAC |
| **hS29_fw** | GGGTCACCAGCAGCTGTACT |
| **hS29_rv** | AAACACTGGCGGCACATATT |
| **hTCF1_fw** | CCCCCAACTCTCTCTCTACGA |
| **hTCF1_rv** | TGCCTGAGGTCAGGGAGTAG |
| **hVEGF_fw** | TGCAGATTATGCGGATCAAACC |
| **hVEGF_rv** | TGCATTCACATTTGTTGTGCTGTAG |

**Supplemental Table 2**

**Human primers used for ChIP-qPCR**

| Primer name | Sequence |
|---|---|
| **hDOT1Lprom_fw** | CCAATAAACAGCATTGTTGTCG |
| **hDOT1Lprom_rv** | CCCACACACGGCTTAGTAAAA |
| **hVEGFprom_fw** | TCACTTTCCTGCTCCCTCCT |
| **hVEGFprom_rv** | GCAATGAAGGGGAAGCTCGA |

**Supplemental Table 3**

**Primers used for the PCR amplification for luciferase assay**

| Construct | Primer | Sequence |
|---|---|---|
| **Full DOT1L promoter (1092 bp)** | Forward | GGTACCTACCTCAGCCCCCGCAGTA |
| | Reverse | ACGCTCGAGGCGGCACTCACGTAGACC |
| **Shorter DOT1L promoter (504 bp)** | Forward | GGTACCCGTGCGTGCGTGGATTCG |
| | Reverse | ACGCTCGAGGCGGCACTCACGTAGACC |

## Supplemental Table 4

## Statistical Analysis Details

| | | | | | | | |
|---|---|---|---|---|---|---|---|
| **FIGURE 3A** | Generalized least square model with constant plus power variance function structure | | | | | | |
| *DOT1L* | beta=0.006, t=6.209 $p$<0.0001 | | | | | | |
| *VEGF* | beta=0.018, t=10.65 $p$<0.0001 | | | | | | |
| **FIGURE 3B** | Generalized least square model with constant plus power variance function structure | | | | | | |
| *DOT1L* | beta=0.015, t=11.14 $p$<0.0001 | | | | | | |
| *VEGF* | beta=0.005, t=24.62 $p$<0.0001 | | | | | | |
| **FIGURE 3C** | Welch-correct unpaired t-test | | | | | | |
| *DOT1L* | $t_2$=4.940 $p$=0.0385 | | | | | | |
| *VEGF* | $t_2$=6.231 $p$=0.0248 | | | | | | |
| **FIGURE 3F** | Generalized least square model | | | | | | |
| *Immuno-fluorescent* | beta=0.007, t=17.32 $p$<0.0001 | | | | | | |
| **FIGURE 4A** | Two-way ANOVA | V:Empty vs. V:DOT1L | V:Empty vs. IOX2:Empty | V:Empty vs. IOX2:DOT1L | V:DOT1L vs. IOX2:Empty | V:DOT1Lvs. IOX2:DOT1L | IOX2:Empty vs. IOX2:DOT1L |
| Luciferase activity | $F_{1,8}$ = 21.71 $p$=0.0016 for IOX2 treatment<br>$F_{1,8}$ = 21.86 $p$=0.0016 for reporter<br>$F_{1,8}$ = 1.38 $p$=0.755 for interaction | $t_8$= 3.078 $p$=0.088 | $t_8$= 3.067 $p$=0.089 | $t_8$= 6.601 $p$=0.001 | $t_8$= 0.0115 $p$=0.99 | $t_8$= 3.522 $p$=0.046 | $t_8$= 3.534 $p$=0.045 |
| **FIGURE 4B** | One-way ANOVA | siSCRv vs. siSCR | siSCRv vs. siHIF1A | siSCRv vs. siHIF2A | siSCR vs. siHIF1A | siSCR vs. siHIF2A | siHIF1A vs. siHIF2A |
| *DOT1L* | $F_{3,8}$ = 36.28 | $t_8$=9.503 $p$<0.0001 | $t_8$=4.426 $p$=0.0132 | $t_8$=8.10 $p$=0.0002 | $t_8$=5.10 $p$=0.0055 | $t_8$=1.427 $p$=0.7207 | $t_8$=3.678 $p$=0.0369 |
| *VEGF* | $F_{3,8}$ = 113.0 | $t_8$=17.25 $p$<0.0001 | $t_8$=10.68 $p$<0.0001 | $t_8$=14.2 $p$<0.0001 | $t_8$=6.57 $p$=0.0011 | $t_8$=3.042 $p$=0.0923 | $t_8$=3.526 $p$=0.0458 |
| **FIGURE 5A** | Linear mixed model | | | | | | |
| *DOT1L* | beta=0.01, t=2.73 $p$=0.046 | | | | | | |
| *VEGF* | beta=0.023, t=15.71, $p$<0.0001 | | | | | | |

| | | | | | | | |
|---|---|---|---|---|---|---|---|
| **FIGURE 5B** | Paired t-test | | | | | | |
| *DOT1L* | $t_2$=3.280 *p*=0.0817 | | | | | | |
| *VEGF* | $t_2$=10.27 *p*=0.0093 | | | | | | |
| **FIGURE 5C** | Linear mixed model | | | | | | |
| *COL2* | beta=0.02, t=4.27, *p*=0.0009 | | | | | | |
| *ACAN* | beta=0.024, t=4.69, *p*=0.0007 | | | | | | |
| **FIGURE 5D** | Paired t-test | | | | | | |
| *COL2* | $t_2$=14.51 *p*=0.0047 | | | | | | |
| *ACAN* | $t_2$=16.84 *p*=0.0035 | | | | | | |
| **FIGURE 5E** | Two-way ANOVA | Vehicle-siSCR vs vehicle-siDOT1L | Vehicle-siSCR vs IOX2-siSCR | Vehicle-siSCR vs IOX2-siDOT1L | Vehicle-siDOT1L v IOX2-siSCR | Vehicle-siDOT1L vs IOX2-siDOT1L | IOX2-siSCR vs IOX2-siDOT1L |
| *COL2* | $F_{1,2}$= 3.378 *p*=0.2075for IOX2 treatment $F_{1,2}$= 9.659 *p*=0.089 for DOT1L silencing $F_{1,2}$= 3.33 *p*=0.2084 for interaction | $t_2$=2.254 *p*=0.6306 | $t_2$=6.480 *p*=0.1303 | $t_2$=1.644 *p*=0.8103 | $t_2$=8.734 *p*=0.0747 | $t_2$=3.898 *p*=0.310 | $t_2$=4.836 *p*=0.218 |
| *ACAN* | $F_{1,2}$= 0.768 *p*=0.4732 for IOX2 treatment $F_{1,2}$= 25.93 *p*=0.0365 for DOT1L silencing $F_{1,2}$= 1.14 *p*=0.3977 for interaction | $t_2$=2.792 *p*=0.496 | $t_2$=1.343 *p*=0.8933 | $t_2$=2.958 *p*=0.461 | $t_2$=4.136 *p*=0.282 | $t_2$=0.1656 *p*=0.9 | $t_2$=4.301 *p*=0.265 |
| *TCF1* | $F_{1,2}$= 31.30 *p*=0.0305 for IOX2 treatment $F_{1,2}$= 80.53 *p*=0.0122 for DOT1L silencing $F_{1,2}$= 8.81 *p*=0.097 for interaction | $t_2$=4.880 *p*=0.215 | $t_2$=3.384 *p*=0.383 | $t_2$=5.694 *p*=0.164 | $t_2$=8.265 *p*=0.083 | $t_2$=0.814 *p*=0.985 | $t_2$=9.079 *p*=0.069 |
| **FIGURE 5F** | Two-way ANOVA | Normoxia-siSCR vs normoxia-siDOT1L | Normoxia-siSCR vs hypoxia-siSCR | Normoxia-siSCR vs hypoxia-siDOT1L | Normoxia- siDOT1 vs hypoxia-siSCR | Normoxia-siDOT1L vs hypoxia-siDOT1L | Hypoxia-siSCR vs hypoxia-siDOT1L |
| *COL2* | $F_{1,2}$= 226.3 *p*=0.0044 for oxygen exposure | $t_2$=3.435 *p*=0.375 | $t_2$=12.68 *p*=0.0364 | $t_2$=9.61 *p*=0.0623 | $t_2$=16.1 *p*=0.0227 | $t_2$=13.04 *p*=0.0344 | $t_2$=3.07 *p*=0.4383 |

| | | | | | | | |
|---|---|---|---|---|---|---|---|
| | $F_{1,2}$= 12.95 *p*=0.069 for DOT1L silencing $F_{1,2}$= 0.07 *p*=0.812 for interaction | | | | | | |
| *ACAN* | $F_{1,2}$= 158.4 *p*=0.0063 for oxygen exposure $F_{1,2}$= 65.75 *p*=0.0149 for DOT1L silencing $F_{1,2}$= 0.012 *p*=0.9225 for interaction | $t_2$=11.0 *p*=0.0476 | $t_2$=15.58 *p*=0.0243 | $t_2$=4.39 *p*=0.2555 | $t_2$=26.6 *p*=0.0083 | $t_2$=15.43 *p*=0.0248 | $t_2$=11.18 *p*=0.0456 |
| *TCF1* | $F_{1,2}$= 2.609 *p*=0.2476 for oxygen exposure $F_{1,2}$= 130.6 *p*=0.0076 for DOT1L silencing $F_{1,2}$= 9.23 *p*=0.093 for interaction | $t_2$=5.945 *p*=0.152 | $t_2$=3.553 *p*=0.357 | $t_2$=6.691 *p*=0.123 | $t_2$=9.50 *p*=0.0637 | $t_2$=0.745 *p*=0.989 | $t_2$=10.24 *p*=0.055 |
| **FIGURE 5G** | Two-way ANOVA | Normoxia V vs. normoxia EPZ | Normoxia V vs hypoxia V | Normoxia-V vs hypoxia EPZ | Normoxia UPZ vs hypoxia V | Normoxia EPZ vs hypoxia EPZ | Hypoxia V vs hypoxia EPZ |
| | $F_{1,2}$= 77.07 *p*=0.0127 for oxygen exposure $F_{1,2}$= 45.62 *p*=0.0212 for EPZ treatment $F_{1,2}$= 16.08 *p*=0.057 for interaction | $t_2$=11.7 *p*=0.0426 | $t_2$=14.55 *p*=0.0278 | $t_2$=8.528 *p*=0.078 | $t_2$=26.2 *p*=0.0087 | $t_2$=20.22 *p*=0.0145 | $t_2$=6.022 *p*=0.1487 |
| **FIGURE 6B** | Kruskal -Wallis | SHAM V vs DMM | | DMM V vs DMM IOX2 | | SHAM V vs DMM IOX2 | |
| OARSI | $\chi^2$=14.297 *p*=0.0008 | Z=3.09 *p*=0.002 | | Z=2.31 *p*=0.021 | | Z=2.41 *p*=0.016 | |
| **FIGURE 6C** | Kruskal -Wallis | SHAM V vs DMM V | | DMM V vs DMM IOX2 | | SHAM V vs DMM IOX2 | |
| osteophyte | $\chi^2$=15.36 *p*=0.0004 | Z=2.71 *p*=0.0068 | | Z=2.22 *p*=0.0267 | | Z=2.71 *p*=0.0068 | |
| **FIGURE 6D** | Kruskal -Wallis | SHAM V vs DMM | | DMM V vs DMM IOX2 | | SHAM V vs DMM IOX2 | |
| synovitis | $\chi^2$=10.93 *p*=0.0064 | Z=2.57 *p*=0.01 | | Z=1.75 *p*=0.08 | | Z=1.13 *p*=0.26 | |
| **FIGURE 6E** | One-way ANOVA | SHAM V vs DMM | | DMM V vs DMM IOX2 | | SHAM V vs DMM IOX2 | |
| HIF1A | $F_{2,12}$=45.45 *p*<0.0001 | $t_{12}$=9.533 *p*<0.0001 | | $t_{12}$=4.909 *p*=0.001 | | $t_{12}$=4.624 *p*=0.0018 | |
| DOT1L | $F_{2,12}$=15.07 *p*=0.0005 | $t_{12}$=4.574 *p*=0.0019 | | $t_{12}$=4.917 *p*=0.001 | | $t_{12}$=0.3435 *p*=0.98 | |
| H3K79 | $F_{2,12}$=45.12 *p*<0.0001 | $t_{12}$=7.792 *p*<0.0001 | | $t_{12}$=8.60 *p*<0.0001 | | $t_{12}$=0.808 *p*=0.82 | |

| **FIGURE S4A** | One-way ANOVA | Vehicle-siSCR vs IOX2-siSCR | Vehicle-siSCR vs IOX2-siHIF1a | Vehicle-siSCR vs IOX2-siHIF2a | IOX2-siSCR vs IOX2-siHIF1a | IOX2-siSCR vs IOX2-siHIF2a | IOX2-siHIF1a vs IOX2-siHIF2a |
|---|---|---|---|---|---|---|---|
| *HIF1A* | $F_{3,8}$ = 77.26 | $t_8$=7.013 *p*=0.0007 | $t_8$=14.80 *p*<0.0001 | $t_8$=4.374 *p*=0.0141 | $t_8$=7.786 *p*=0.0003 | $t_8$=2.639 *p*=0.1659 | $t_8$=10.42 *p*<0.0001 |
| *HIF2A* | $F_{3,8}$ = 191.4 | $t_8$=3.203 *p*=0.0725 | $t_8$=0.4094 *p*=0.9992 | $t_8$=18.36 *p*<0.0001 | $t_8$=3.617 *p*=0.0402 | $t_8$=21.57 *p*<0.0001 | $t_8$=17.96 *p*<0.0001 |
| **FIGURE S5A** | Two-way ANOVA | Vehicle-siSCR vs vehicle-siDOT1L | Vehicle-siSCR vs IOX2-siSCR | Vehicle-siSCR vs IOX2-siDOT1L | Vehicle-siDOT1L v IOX2-siSCR | Vehicle-siDOT1L vs IOX2-siDOT1L | IOX2-siSCR vs IOX2-siDOT1L |
| *DOT1L* | $F_{1,2}$= 7.730 *p*=0.1087 for IOX2 treatment $F_{1,2}$= 140.9 *p*=0.0070 for DOT1L silencing $F_{1,2}$= 0.7453 *p*=0.4789 for interaction | $t_2$=9.986 *p*=0.0578 | $t_2$=2.150 *p*=0.6601 | $t_2$=9.057 *p*=0.0697 | $t_2$=12.14 *p*=0.0397 | $t_2$=0.9286 *p*=0.9727 | $t_2$=11.21 *p*=0.0463 |
| **FIGURE S5B** | Two-way ANOVA | Normoxia-siSCR vs normoxia-siDOT1L | Normoxia-siSCR vs hypoxia-siSCR | Normoxia-siSCR vs hypoxia-siDOT1L | Normoxia-siDOT1L vs hypoxia-siSCR | Normoxia-siDOT1L vs hypoxia-siDOT1L | Hypoxia-siSCR vs hypoxia-siDOT1L |
| *DOT1L* | $F_{1,2}$= 12.32 *p*=0.0725 for oxygen exposure $F_{1,2}$= 91.27 *p*=0.0108 for DOT1L silencing $F_{1,2}$= 0.06641 *p*=0.8207 for interaction | $t_2$=9.809 *p*=0.0599 | $t_2$=2.292 *p*=0.6201 | $t_2$=7.153 *p*=0.1087 | $t_2$=12.10 *p*=0.0399 | $t_2$=2.656 *p*=0.5270 | $t_2$=9.445 *p*=0.0644 |

64